

Integrating Capacitive Energy Storage (CES) into Existing Power System to Manage Frequency Deviation

Kanika Wadhwa¹, S. K. Gupta²

Submitted: 22/06/2023

Revised: 05/08/2023

Accepted: 24/08/2023

Abstract: This paper attempts to demonstrate the use, design, and performance analysis of a new Black Widow optimized (BWO) controller for automatic generation control (AGC) of connected two-area reheat thermal power systems considering renewable energy sources with energy storage. Using BWO, the controller's parameters are established. Power system models incorporate fast-acting energy storage units such as redox flow batteries (RFBs) and Capacitive energy storage (CES), and their effectiveness in improving AGC performance is tested and compared. After examining the controller's performance in a multi-area thermal-hydro-gas power system, the research is expanded to include a proposed model with RES. The findings of a MATLAB simulation show that the system's dynamic performance is enhanced when RFB and CES are present.

Keywords: Black Widow Optimization, Capacitive Energy Storage, Redox Flow Battery, Renewable Energy Source

1. Introduction

A power utility's primary goals are the cost-effective and expert generation (G), transmission (T), distribution (D), and control of electrical power and the maintenance of a reliable and acceptable energy supply for users. Automatic generation control is essential to the efficient operation of the power system in order to maintain a constant supply of high-quality electricity (AGC) [1]. The mismatch between load demand and generation is shown by frequency deviation (FD), which is connected to power quality problems. In response to consumer load requirements and disturbances, AGC regulates production, demand, and losses to maintain safe levels of FD and tie-line power (delP_{tie}) flows [2]. AGC regulates production, demand, and losses to maintain safe levels of FD and tie-line power (delP_{tie}) flows.

Therefore, researchers are making an effort to propose new AGC control structures for use in power grids. The generating unit is equipped with a pair of controllers under the governance of the governor. The main control mechanism exhibits rapid response, whereas the secondary control mechanism has a slower reaction time. Secondary controller design has been at the forefront of recent LFC studies. The proportional integral derivative (PID) controller was used as the SC in the LFC research by the authors of [3]–[5]. Saikia et al. [6] investigated the differences between the I, PI, PID, ID, and I double D (IDD) classical controllers for systems with a single degree of

freedom (1-DOF). IDD controller outperforms ID, PID, PI, and I controllers, according to studies cited in [6]. Two degrees of freedom proportional integral derivative (2-DOF-PID) controller as SC was introduced by Raju et al [7].

Reviewing the relevant literature indicates that people have tried to offer various control approaches. Conventional LFC uses many different optimization methods, such as genetic algorithms [8]–[10], craziness-based particle swarm optimization [11], firefly [12], [13], bacterial foraging [14]–[16], particle swarm optimization [17], whale optimization [18], and differential evolution [19], [20], to fine-tune the SC gains and their associated parameters. In addition to classical optimal PI [1], [2], grey wolf optimization [21], ICA based PID [5], genetic algorithm (GA)-based different controller [22], [23], and BBBO-based controller (PI) [24], the literature review reveals the introduction of numerous development and research strategies related to controllers for various types of PS models.

System dynamics are improved when CES and RFB are used together in PS, as shown by an analysis of the impacts of ESSs. [25]. RES in PS displays intermittent generation, and the loss of inertia worsens PS stability. Examples of RES in PS include solar and wind. With this inertial decrease and the random nature of power generation and load demand in modern PS, LFC has become a vital competition compared to traditional PS. A sensible, fast answer ESD makes the PS more stable by adding storage space, which balances out the sudden change in load. Energy storage systems (ESSs) are installed in PS to boost the AGC's functionality. ESSs can quickly and precisely respond to power surges and drops, compensating for these fluctuations in various situations. They also aid electricity quality by reducing FD on the grid.

¹DCRUST, Murthal, Sonapat, Haryana, 131001, India
ORCID ID : 0000-0003-3914-1962

²DCRUST, Murthal, Sonapat, Haryana, 131001, India
ORCID ID : 0000-0002-5120-5028

* Corresponding Author Email: 18001902002kanika@dcrustm.org

Here are some of the key innovations and methods used in this work:

1. To demonstrate the superiority of the BWO-based PID controller over the PSO-PI, PSO-PI with derivative (PID), AEFA-PI, AEFA-PID, hAEFA-PI, and hAEFA-PID structured controllers for solving the LFC problem

in a 2-area Reheat thermal hydro gas (RTHG)-Power system.

2. Optimizing the PID controller's settings with the BWO algorithm after incorporating a redox flow battery and a capacitive

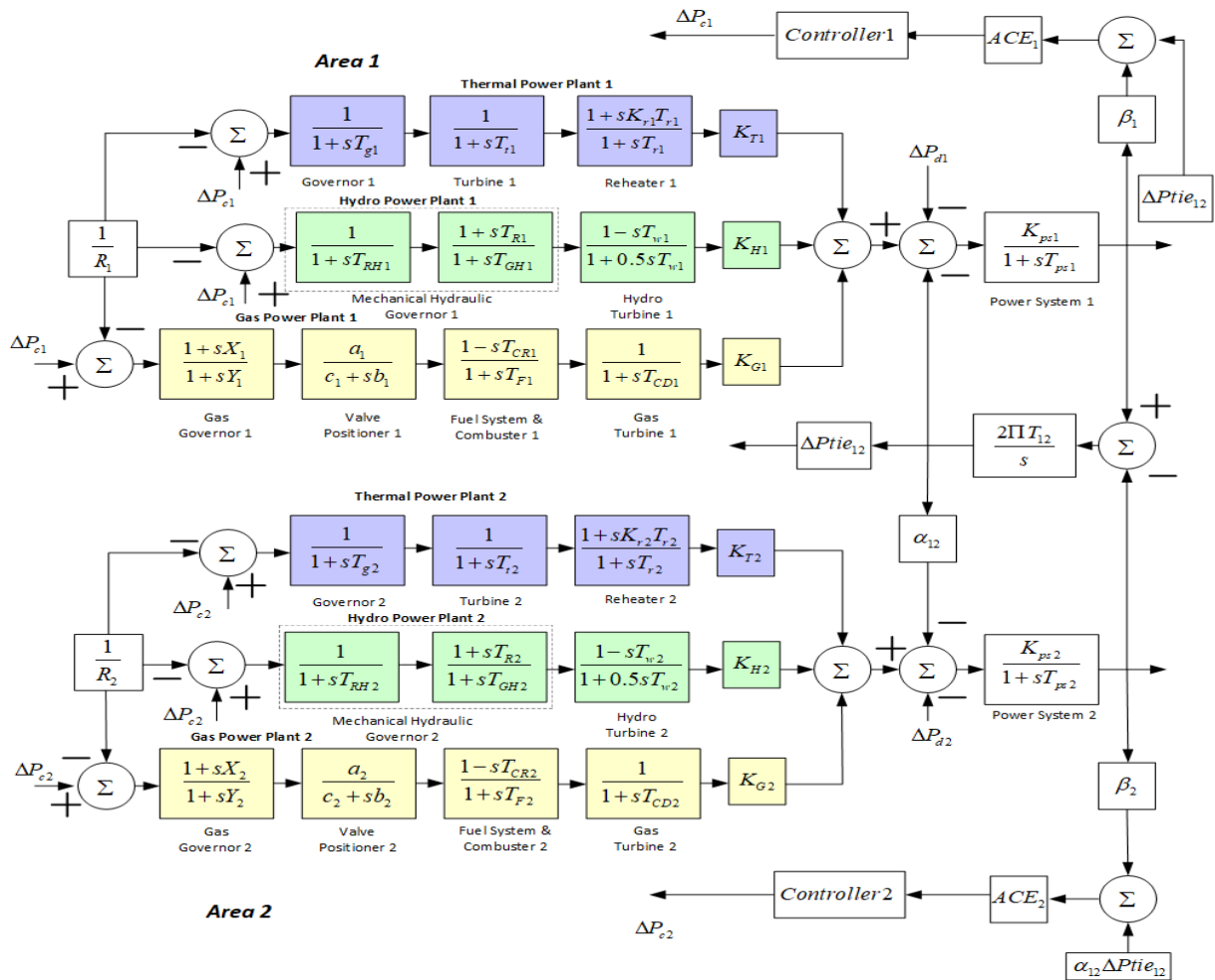


Fig 1. MSTHG Power System

energy storage system into a two-area reheat thermal-hydro-gas power system.

3. To demonstrate that the proposed FPIDN (1+PI) controller outperforms enhanced PID controllers, and to generalize the work to a two-area hybrid power system (Thermal-Hydro-Gas-Wind-Solar (THGWS)) that makes use of capacitive energy storage.

2. PS Model

The researched PSs are shown in Figures 1 and 2, and they are the Multisource Two Area Thermal-Hydro-Gas (MSTHG) PS and the Multisource Two Area Thermal-Hydro-Gas-Solar-Wind (MSTHGSW) PS. Each control region of the MSTHG system has one reheat thermal, one hydro (mechanical governor), and one gas PS. The MSTHGSW system contains one reheat thermal, one Hydro, one Gas, one Solar, and one Wind PS for each

control area. For the purposes of this research, we will be concentrating on a hybrid source power model for a two-area power system plant that utilizes hydro, thermal, and gas generation. There are three generators in each zone, and their transfer function models are shown in Figure 1.

The rated power in megawatts (MW) for each of Areas 1 and 2 is denoted by Pr1 and Pr2, respectively. In MSTHGSW Power System model represents in figure 2.

Assume that $K_{t1}, K_{h1}, K_{w1}, K_{g1}$, and K_{s1} represent the proportions of thermal, hydro, wind, gas, and solar sources, respectively, in the power generation for area-1. In area-1, $P_{Gt1}, P_{Gh1}, P_{Gw1}, P_{Gg1}$ and P_{Gs1} are the generations in MegaWatt produced by thermal, hydro, wind, gas, and solar sources, respectively

3. Controller

A well-known and effective controller is the fuzzy logic controller (FLC). There has been a recent uptick in the usage of FLC in studies due to its ease of implementation and superior results. When compared to the standard controller, FLC provides more versatility. There are five main parts to

every MF-based fuzzy inference system: fuzzifying the input signals, executing the (Or and AND) fuzzy operator in the antecedent, applying the antecedent to the consequent, accumulating the consequent with a rule base, and finally defuzzifying the system.. FLC is made up of an operator-tested "if-then" rule set. Figure3 outlines the layout of

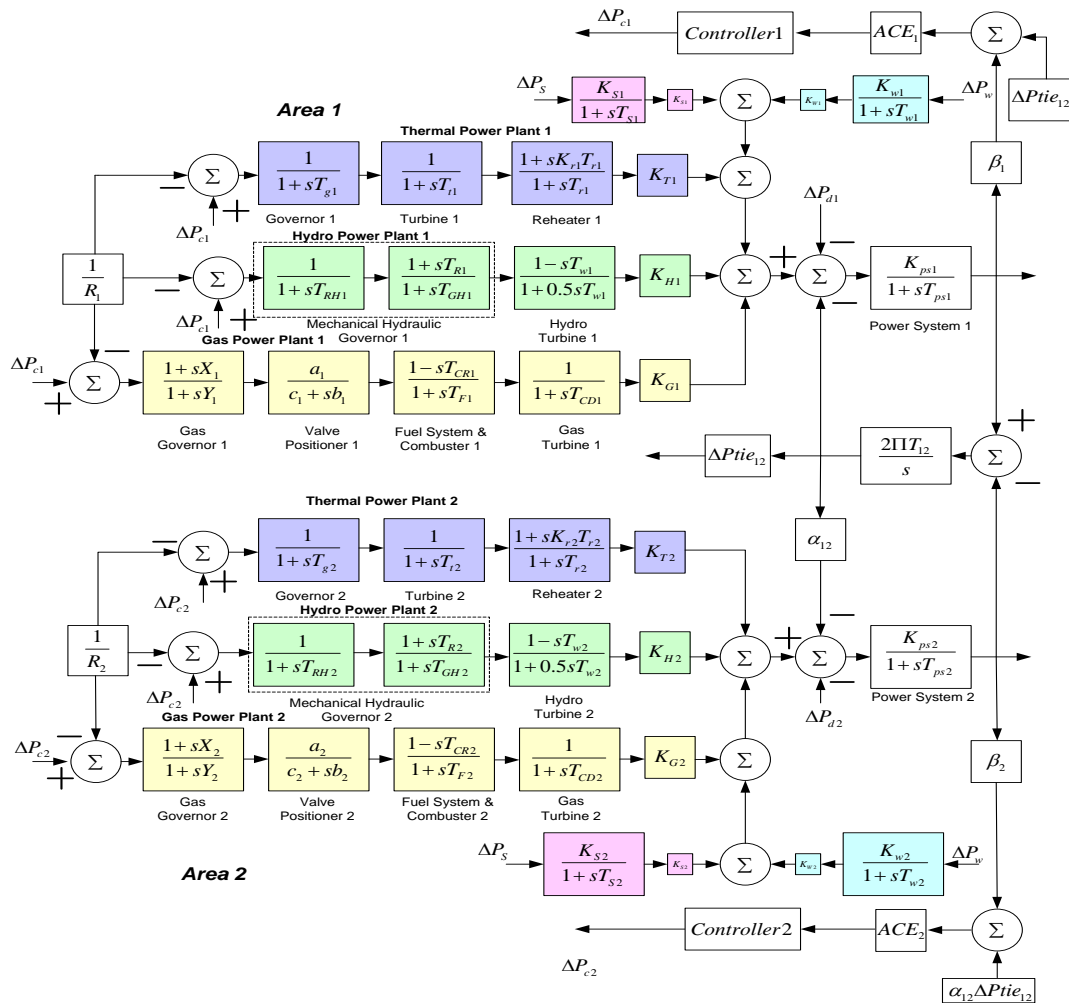


Fig 2. MSTHGWS Power System

the FPIDF-(1 + PI) controller. Specifically, the FLC takes as inputs the area control error (ACE) and its derivative.

Controller with FPIDF(1+PI) has Dual-input fuzzy logic controller. Both ACE and a derivative of ACE are taken as inputs. The FLC's output goes into the PIDF controller, and the PIDF's output goes into the 1+PI controller. This controller is taken from[26].

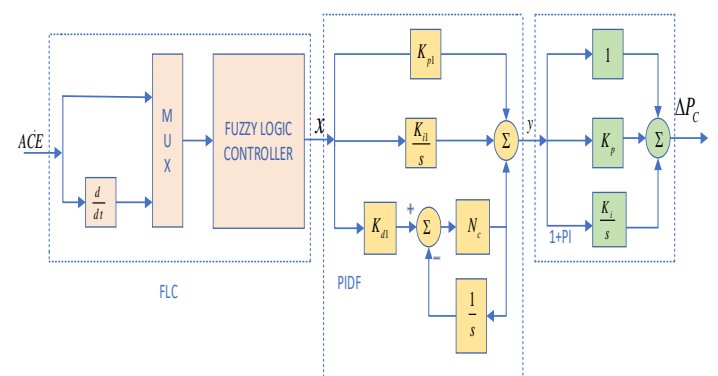


Fig 3. FPIDF-(1+PI) Controller

4. Black Widow Optimization

The hunting behaviour of black widow spiders inspired the Black Widow Optimization Algorithm (BWOA), which is a

meta - heuristic optimization algorithm. It was proposed as a swarm intelligence algorithm for solving complex optimization problems. The BWOA is a population-based algorithm that simulates the interactions between male and female black widow spiders during the mating process. In the algorithm, each potential solution to the optimization problem is represented as a spider in the population. The spiders interact and move in the search space to find the optimal solution.

Where N is no. of widows and D is the size of a problem that needs to be solved.

In the population, $X_i = [x_{i,1}, x_{i,2}, \dots, x_{i,D}] (1 \leq i \leq N)$ represents the *i*th widow. Each element in individual $X_i = [x_{i,1}, x_{i,2}, \dots, x_{i,D}] (1 \leq i \leq N)$ is initialized by Equation (1).

$$X_{i,j} = L_j + (U_j - L_j) \cdot rand(0,1), (1 \leq j \leq D) \quad (1)$$

In the optimization model, the lower and upper limits of the variables are $L = [l_1, l_2, \dots, l_D]$, $U = [u_1, u_2, \dots, u_D]$

4.2. Procreate

Black widows have a special way of reproducing their offspring. When mating begins, spiders with the highest procreation rates (Pp) are chosen at random from the population to act as parents to their offspring. Equation (2) causes the offspring to be born.

$$\begin{cases} Y_i = \alpha X_i + (1 - \alpha) X_j \\ Y_j = \alpha X_j + (1 - \alpha) X_i \end{cases} \quad (2)$$

where X_i and X_j represent a spider's mother and father.

The progeny of this pairing are Y_i and Y_j and α represents a D-dimensional array of random integers between [0 1].

4.3. Cannibalism

Sexual cannibalism, cannibalism between siblings, and cannibalism between children and their mother are all part of this stage. The best spiders can be kept alive by culling the average ones.

a). Sexual Cannibalism

During or after mating, the female black widow will devour her spouse. Female spiders that make it to the following

There are four steps to the BWO algorithm: population seeding, procreation (reproduction), cannibalism, and mutation.

4.1. Initialization

spider population is

$$W_{N \times D} = [X_1, X_2, \dots, X_N]$$

generation are selected for survival.

b). Cannibalism between siblings

Due to competition for food or predators, the strongest spiders would consume their younger siblings to ensure their survival. A spider's resilience may be measured by its fitness value. The amount of people that make it through this process is based on a parameter called the cannibalism rating (CR).

c). Cannibalism between children and their mother

It's possible that a very large offspring may consume its mother spider. That is to say, if a mother and father produce a solution that has a high fitness value, the offspring will eventually replace the mother.

4.4. Mutation

In this phase, the mutation rate (Pm), which is a constant, determines how many entities in the population undergo mutation.

Two array elements, $x_{i,m}$ and $x_{i,n}$ ($1 \leq m, n \leq D$), are chosen at random for the selected individual $X_i (1 \leq i \leq N)$, and then switched places. As can be seen in Figure 3, the new individuals undergo unpredictable shifts in fitness.

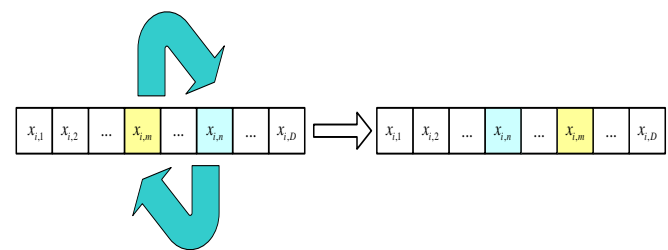


Fig 4. Mutation

Flow Chart of BWO is shown in Fig. 5

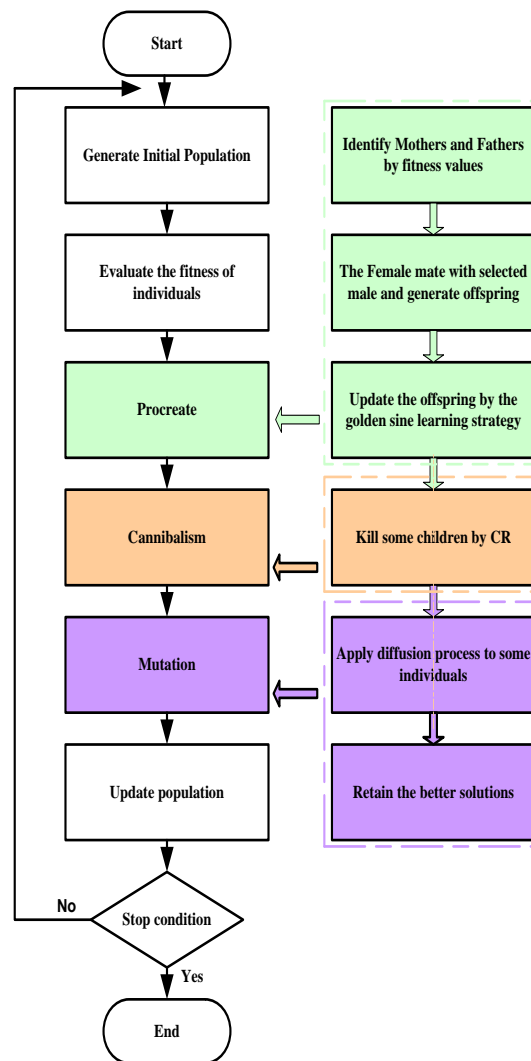


Fig 5. Flow Chart of BWO

Table 1. Optimum values of controller parameters for MSTHG PS

	Kp1	Ki1	Kd1	Kp2	Ki2	Kd2	ISE X 10 ⁻³
BWO-PID	-4.1751	-4.4138	-1.7201	-4.1702	-3.3506	-2.9209	0.1134
PSO-PI	0.451	0.2514	-	0.4518	0.2514	-	1.8531
AEFA-PI	1.392	0.9741	-	1.3920	0.9741	-	1.5874
HAEFA-PI	1.970	1.2654	-	1.9702	1.2654	-	1.4146
PSO-PID	0.951	0.7500	0.2500	0.9516	0.7500	0.2500	1.6813
AEFA-PID	2.917	1.7541	0.6891	2.9176	1.7541	0.6891	1.3754
HAEFA-PID	3.7141	2.7167	1.3491	3.7141	2.7167	1.3491	1.0188

Table 2. Comparative performance of ISE value and settling times for MSTHG PS

	Settling Time (s)			ISE X 10 ⁻³
	delF1	delF2	delPtie	
Proposed BWO tuned PID	3.7587	5.7664	2.5995	0.1134
PSO-PI[28]	32.46	28.39	28.44	1.8531
AEFA-PI[28]	26.36	25.46	26.94	1.5874
HAEFA_PI[28]	22.47	24.53	24.91	1.4146
PSO-PID[28]	21.66	23.31	24.28	1.6813
AEFA-PID[28]	19.58	21.80	23.05	1.3754
HAEFA-PID[28]	14.07	19.03	18.33	1.0188

5. Energy Storage System

Minor step load disruptions occur regularly in linked PSs. Thus, fluctuations in frequency, tie-line power, and power production occur consistently, albeit for brief periods. The governor may fail to control the errant signal under dynamic conditions because of its slow action and the system's nonlinearities. So, to meet demand and make system more stable, it's essential to use ESSs like CES and RFB that can respond more quickly in the control areas of PS.

5.1. Capacitive Energy Storage

CES devices are getting a lot of attention in both theory and actual studies because they have a lot of uses in current power systems. They may be able to mitigate system transients such as low-frequency power fluctuations and frequency shifts. CES's many advantages include its rapid charging and discharging without losing efficiency, its high-power density, its quick response time, its long working life, its ability to supply the grid with power during times of high or intermittent demand, its lack of maintenance requirements, its positive impact on the environment, its simplicity and low cost, etc.[26], [27]. The CES unit is made up of a supercapacitor, a power conversion system (PCS), and safety electronics.[27]. CES units hold energy when not being used and send it to the grid instantly via PCS when there is a sudden load demand. To ensure that the power system's dynamic performance increases and that frequency and tie line power errors are reduced, CES units are incorporated into both domains of the power system models under investigation. Power changes per CES increment are expressed as:

$$\Delta P_{CS_i} = \left\{ \left[\frac{K_{CS}}{1+sT_{CS}} \right] \left[\frac{1+sT_a}{1+sT_b} \right] \left[\frac{1+T_c}{1+T_d} \right] \right\} \Delta F_i$$

Table 3. Percentage improvement of ISE for MSTHG PS

Optimization Technique	Improved percentage
PSO-PI[28]	93.88
AEFA-PI[28]	92.85
HAEFA_PI[28]	91.98
PSO-PID[28]	93.25
AEFA-PID[28]	91.75
HAEFA-PID[28]	88.86

Table 4. Optimum values of controller parameters for MSTHG PS with ESS

	Kp1	Ki1	Kd1	Kp2	Ki2	Kd2	ISE X 10 ⁻³
BWO	-4.1751	-4.4138	-1.7201	-4.1702	-3.3506	-2.9209	0.1134
BWO-CES	-6.9275	-6.7110	-6.7095	-3.8437	-2.6196	-3.9121	0.0195
BWO-CES-RFB	-6.6824	-6.6639	-6.5134	-3.6833	-3.7806	-3.9349	0.0142

where the time constants for the phase compensator blocks are Ta, Tb, Tc, and Td for i=1 and 2 respectively. The time constant and gain of CES are denoted by TCS and KCS. ΔF is the FD of area. A central CES unit receives the ΔF signal from each region and produces the required amount of ΔF -related electricity.

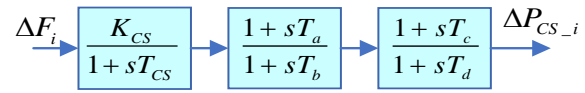


Fig 6. TF Model for CES

5.2. Redox Flow Battery

The redox flow battery (RFB) is now one of the most powerful and quickly rechargeable batteries. RFB's primary selling points are its scalability, flexibility, adaptability, emancipated power capacity, tremendous efficiency, low environmental impact, etc. RFB outperforms the other ESSs and is the best at increasing frequency stability. RFB is a practical choice due to its long lifespan, low operating losses, and ease of maintenance. RFB stores energy during periods of low demand and releases it immediately in response to spikes in use. When it comes to the AGC problem, the FD signal is sent into the RFB integrated in both control areas of the two-area systems.

The variation in RFB power for SLP is expressed as

$$\Delta P_{RFB_i} = \left[\frac{K_{RFB_i}}{1+sT_{RFB_i}} \right] \Delta F_i$$

where T_{RFB_i} and K_{RFB_i} represent the RFB's time constant and gain, respectively.

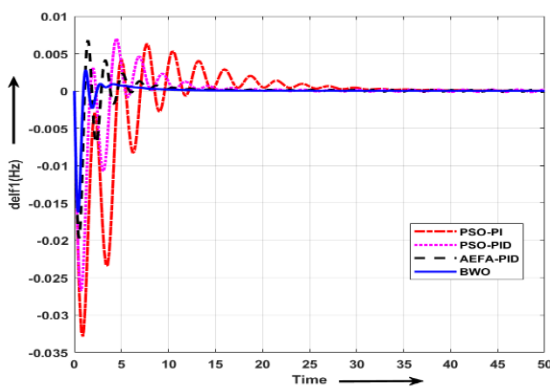
Table 5. Comparative performance of ISE value and settling times for MSTHG PS with ESS

	Settling Time (s)			ISE X 10 ⁻³
	delF1	delF2	delPtie	
Proposed BWO tuned PID	3.7587	5.7664	2.5995	0.1134
BWO-CES	3.4653	5.6832	2.4236	0.0195
BWO-CES-RFB	3.3246	4.8692	1.9456	0.0142

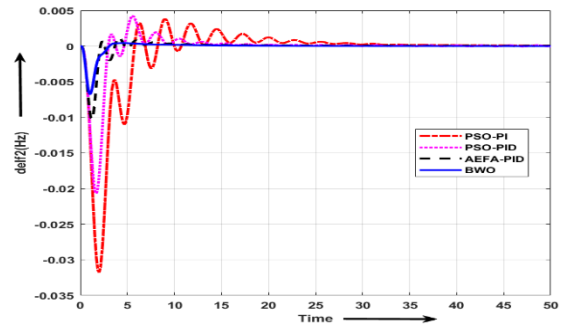
6. Simulation Outcome

6.1. MSTHG power system analysis for 1% SLP in area 1

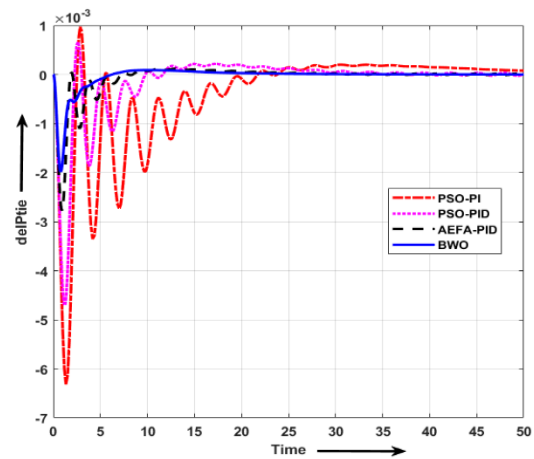
To further dampen frequency oscillations, a full study of the investigated linked system is next performed using the PID controller. Fig. 7 shows how the system responds for the system MSTHG, and the reactions are calculated based on the settling time shown in Table 2. The numerical and graphical results reveal that the suggested BWO algorithm works well with the PID controller when compared to existing methods. A two-area, three-unit power system model demonstrates how well the BWO-optimized PID controller can manage multi-area power systems. One thermal plant, one hydro plant, and one gas plant are provided in each region. Fig. 1 displays the TF model for the combined thermal, hydro, and gas power plant. In addition to the given BWO technique, several optimisation strategies are available in recent literature for optimising the conventional PI/PID controllers. Using a 1% SLD at $t = 0$ s in area-1, the resulting F1, F2, and Ptie12 are shown in Fig. 7. We then evaluate the outcomes in comparison to the existing PSO, hAEFA, and AEFA algorithms. Table 1 displays the numerical findings. Improvement of the objective function (ISE) considering MSTHG with BWO is shown in Table 3.



a. FD in area 1



b. FD in area 2



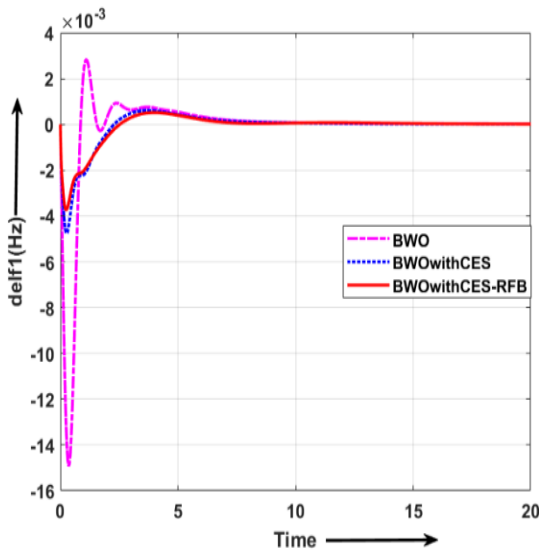
c. Tie-line Power Deviation

Fig 7. Responses of MSTHG considering 1% SLP in area 1

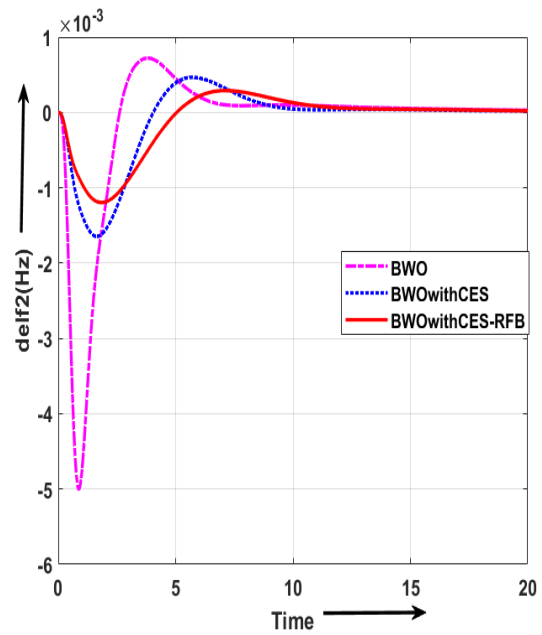
6.2. MSTHG power system considering Energy Storage System

The suggested controller is instigated using a two-area power grid and a hybrid generating station equipped with CES and CES-RFB. The fig. 2 displays the TF model of the system. Under a load disturbance of 1% puMW in area 1 ($delPd1 = 0.01$ puMW) at $t = 0$ sec, the two-area hybrid model is simulated using a PID, FPIDN(1+PI) controller. The effectiveness of the BWO-optimized PID-CES-RFB controller is compared to that of the BWO-optimized PID-CES controller and the BWO-tuned PID controller. Graphical and tabular displays of the data demonstrate the efficacy of CES/CES-RFB in reducing PS fluctuations at SLP. Results are shown in Fig. 8. Table 5 gives the calculated values for JISE and TS (settling time) of the

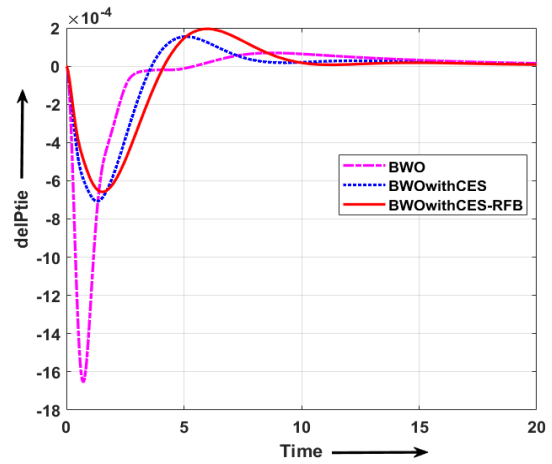
delF1/delF2/delPtie12. Results show least JISE (0.0142 X 10⁻³) with PID controller with CES_RFB, and they quickly settle to their desired value of zero in minimal settling time.



a. FD in area 1



b. FD in area 2



c. Tie-line Power Deviation

Fig 8. Responses of MSTHG considering ESS

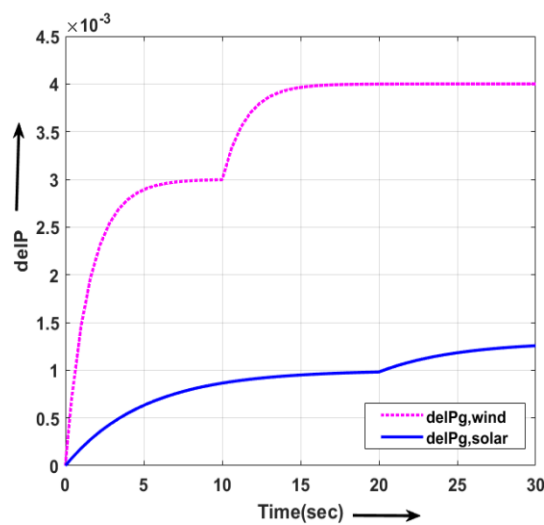


Fig 9. Solar Power and Wind Power

Table 6. Optimum values of controller parameters for MSTHGSW PS with ESS

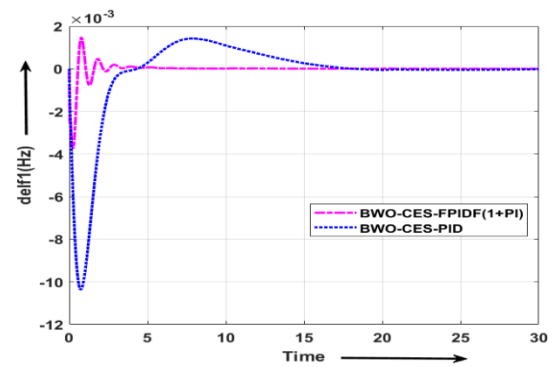
	Kp1	Kp2	Ki1	Ki2	Kd1	Kd2	N	Kp	Ki	ISE
BWO_PIDwith CES	-1.7774	-1.5936	-1.7194	-0.9677	-1.7186	-1.5191	100	-	-	2.2072×10^{-3}
BWO-FPIDF(1+PI)with CES	2.2467		9.8642		0.1352		100.5328	2.1351	0.0234	5.4020×10^{-6}

Table 7. Comparative performance of ISE value and settling times for MSTHGSW PS with ESS

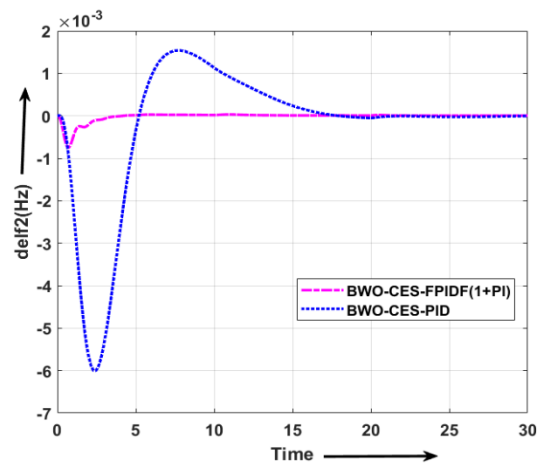
	delF1	Settling Time (s)		ISE
		delF2	delPtie	
BWO_PIDwith CES	13.36	14.54	6.37	2.2072×10^{-3}
BWO-FPIDF1+PIwith CES	2.0490	3.3520	3.8546	5.4020×10^{-6}

6.3. MSTHG Power System with RES and ESS

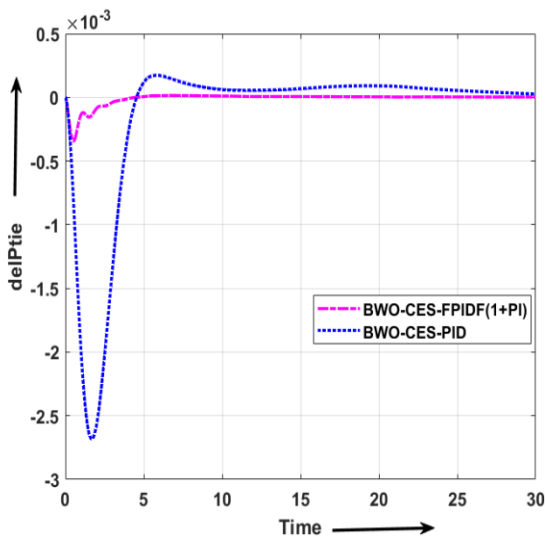
MSTHG PS with solar and wind power systems in both areas, as shown in the fig. 2 named as MSTHGSW, is modeled with 1% load disturbance applied in area 1, i.e., $P_{D1} = 0.01$ pu MW. Solar Power and Wind Power is taken from [25] and showed in figure 8. Solar power change at 20 s and Wind Power change at 10 s. The Fig. 10 displays the system's response to FD in area 1, FD in area 2, Change in tie-line power using a BWO-optimized PID controller with CES and a BWO-optimised FPIDF (1+PI) with CES, respectively. The BWO-optimized FPIDF (1+PI) controller yields superior response speed, undershoot, and settling time (as determined by the parameters F1, F2, and Ptie12). The performance of the controller is enhanced when CES units are put in both PS zones because active power is delivered in addition to the power generated by the turbine inertia at the time of SLP application. In contrast to the PID controller using CES units, the system's performance is much improved by using the recommended FPIDF-(1 + PI) controller. Table 7 gives the calculated values for settling time and objective function of the delF1/delF 2/delPtie12 . Results show least JISE (5.4020×10^{-6}) with FPIDF-(1 + PI) controller with energy storage (CES), and fast reach their intended value of zero in minimal T_s .(F 1 = 2.04 s, F 2 = 3.35 s, Ptie12 = 3.85 s) compared to J_{ISE} (2.2072×10^{-3}), and T_s (F 1 = 13.36 s, F 2 = 14.54 s, Pt= 6.37 s) values offered by the PID controller with energy storage (CES).



a. FD in area 1



b. FD in area 2



c. Tie-line Power Deviation

Fig 10. Responses of MSTHGSW considering 1% SLP in area 1

7. Conclusion

In this insightful analysis, we compare and contrast the effectiveness of CES and united RFB/CES in advancing AGC behavior for two-area conventional PS. Using a BWO-optimized FPIDF(1 + PI) controller effectively solves the AGC issue in PS. The effectiveness of this controller was validated on a common two-area traditional reheat thermal system that used hydro, gas, solar, and wind energy sources.

These are the key takeaways from the study:

1. Compared to PI, PID, and designed controllers optimised using a variety of currently-published optimisation approaches, the performance of a BWO-optimised PID controller is superior in terms of the lowest values of settling time and objective function
2. The performance of PID with CES+RFB is superior to that of PID without CES and PID with CES. Thus, CES and RFB considerably dampen system oscillations after a disturbance in the control region.
3. Renewable energy sources (RES) and energy storage systems (ESS) are included in the investigated models to evaluate their effects.
4. When RFB and CES are combined in the control domains, the best system results are achieved with the FPIDF-(1+PI) controller by reducing system frequency/tie-line power flow variations.

References

[1] Y. Arya, N. Kumar, and S. K. Gupta, "Optimal automatic generation control of two-area power systems with energy storage units under deregulated

environment," *Journal of Renewable and Sustainable Energy*, vol. 9, no. 6, Nov. 2017.

- [2] P. Dahiya, P. Mukhija, A. R. Saxena, and Y. Arya, "Comparative performance investigation of optimal controller for AGC of electric power generating systems," <https://doi.org/10.7305/automatika.2017.12.1707>, vol. 57, no. 4, pp. 902–921, 2018.
- [3] W. Tan, "Unified tuning of PID load frequency controller for power systems via IMC," *IEEE Transactions on Power Systems*, vol. 25, no. 1, pp. 341–350, Feb. 2010.
- [4] E. S. Ali and S. M. Abd-Elazim, "BFOA based design of PID controller for two area Load Frequency Control with nonlinearities," *International Journal of Electrical Power & Energy Systems*, vol. 51, pp. 224–231, Oct. 2013.
- [5] H. Shabani, B. Vahidi, and M. Ebrahimpour, "A robust PID controller based on imperialist competitive algorithm for load-frequency control of power systems," *ISA Trans*, vol. 52, no. 1, pp. 88–95, Jan. 2013.
- [6] L. C. Saikia, N. Sinha, and J. Nanda, "Maiden application of bacterial foraging based fuzzy IDD controller in AGC of a multi-area hydrothermal system," *International Journal of Electrical Power & Energy Systems*, vol. 45, no. 1, pp. 98–106, Feb. 2013.
- [7] M. Raju, C. Saikia, and N. Sinha, "Load Frequency Control of Multi-area Hybrid Power System Using Symbiotic Organisms Search Optimized Two Degree of Freedom Controller," 2017.
- [8] Y. L. Abdel-Magid and M. M. Dawoud, "Optimal AGC tuning with genetic algorithms," *Electric Power Systems Research*, vol. 38, no. 3, pp. 231–238, Sep. 1996.
- [9] Z. M. Al-Hamouz and H. N. Al-Duwaish, "A new load frequency variable structure controller using genetic algorithms," *Electric Power Systems Research*, vol. 55, no. 1, pp. 1–6, Jul. 2000.
- [10] S. Panda and N. K. Yegireddy, "Automatic generation control of multi-area power system using multi-objective non-dominated sorting genetic algorithm-II," *International Journal of Electrical Power & Energy Systems*, vol. 53, no. 1, pp. 54–63, Dec. 2013.
- [11] H. Gozde and M. C. Taplamacioglu, "Automatic generation control application with craziness based particle swarm optimization in a thermal power system," *International Journal of Electrical Power & Energy Systems*, vol. 33, no. 1, pp. 8–16, Jan. 2011.
- [12] N. Manoharan, S. S. Dash, and K. S. Rajesh, "Load Frequency Control of Nonlinear Power System Employing Firefly Algorithm," *Indian J Sci Technol*, vol. 10, no. 13, pp. 1–6, Apr. 2017.
- [13] R. K. Sahu, S. Panda, and S. Padhan, "A hybrid firefly algorithm and pattern search technique for automatic

- generation control of multi area power systems,” *International Journal of Electrical Power & Energy Systems*, vol. 64, pp. 9–23, Jan. 2015.
- [14] S. K. Gupta, K. Wadhwa, and J. Raja, “BF Optimized Controllers for Three Area H-T-H System Under Deregulated Environment,” 2012, Accessed: Nov. 23, 2022. [Online].
- [15] S. Kumar, K. Wadhwa, and S. K. Gupta, “Enhancing the performance of multi area AGC in deregulated environment tuned with TCPS Using BFO,” *PIICON 2020 - 9th IEEE Power India International Conference*, Feb. 2020.
- [16] K. Wadhwa, J. Raja, and S. K. Gupta, “BF based integral controller for AGC of multiarea thermal system under deregulated environment,” 2012 IEEE 5th Power India Conference.
- [17] Y. L. Abdel-Magid and M. A. Abido, “AGC tuning of interconnected reheat thermal systems with particle swarm optimization,” *Proceedings of the IEEE International Conference on Electronics, Circuits, and Systems*, vol. 1, pp. 376–379, 2003.
- [18] K. S. Simhadri, B. Mohanty, and S. K. Panda, “Comparative performance analysis of 2DOF state feedback controller for automatic generation control using whale optimization algorithm,” *Optim Control Appl Methods*, vol. 40, no. 1, pp. 24–42, Jan. 2019.
- [19] U. K. Rout, R. K. Sahu, and S. Panda, “Design and analysis of differential evolution algorithm based automatic generation control for interconnected power system,” *Ain Shams Engineering Journal*, vol. 4, no. 3, pp. 409–421, Sep. 2013.
- [20] M. K. Debnath, R. K. Mallick, and B. K. Sahu, “Application of Hybrid Differential Evolution–Grey Wolf Optimization Algorithm for Automatic Generation Control of a Multi-Source Interconnected Power System Using Optimal Fuzzy–PID Controller,” *Electric Power Components and Systems*, vol. 45, no. 19, pp. 2104–2117, 2017.
- [21] D. Guha, P. K. Roy, and S. Banerjee, “Load frequency control of interconnected power system using grey wolf optimization,” *Swarm Evol Comput*, vol. 27, pp. 97–115, Apr. 2016.
- [22] K. R. M. Vijaya Chandrakala, S. Balamurugan, and K. Sankaranarayanan, “Variable structure fuzzy gain scheduling based load frequency controller for multi source multi area hydro thermal system,” *International Journal of Electrical Power & Energy Systems*, vol. 53, no. 1, pp. 375–381, Dec. 2013.
- [23] C. Ismayil, R. Sreerama Kumar, and T. K. Sindhu, “Automatic Generation Control of Single Area Thermal Power System with Fractional Order PID (PI λ D μ) Controllers,” *IFAC Proceedings Volumes*, vol. 47, no. 1, pp. 552–557, Jan. 2014.
- [24] D. Guha, P. K. Roy, and S. Banerjee, “Blended biogeography based optimization based LFC controller applied to multi-unit,” *IET Conference Publications*, vol. 2015, no. CP683, pp. 143–149, 2015.
- [25] Y. Arya, “Effect of energy storage systems on automatic generation control of interconnected traditional and restructured energy systems,” *Int J Energy Res*, vol. 43, no. 12, pp. 6475–6493, Oct. 2019.
- [26] S. Dhundhara and Y. P. Verma, “Capacitive energy storage with optimized controller for frequency regulation in realistic multisource deregulated power system,” *Energy*, vol. 147, pp. 1108–1128, Mar. 2018.
- [27] Y. Arya, “AGC of PV-thermal and hydro-thermal power systems using CES and a new multi-stage FPIDF-(1+PI) controller,” *Renew Energy*, vol. 134, pp. 796–806, Apr. 2019,.
- [28] C. Kalyan, G. R.-I. J. on Electrical, and undefined 2020, “Coordinated SMES and TCSC Damping Controller for Load Frequency Control of Multi Area Power System with Diverse Sources,,” *pdfs.semanticscholar.org*, vol. 12, no. 4, 2020.
- [29] Singh, J. ., Mani, A. ., Singh, H. ., & Rana, D. S. . (2023). Quantum Inspired Evolutionary Algorithm with a Novel Elitist Local Search Method for Scheduling of Thermal Units. *International Journal on Recent and Innovation Trends in Computing and Communication*, 11(3s), 144–158. <https://doi.org/10.17762/ijritcc.v11i3s.6175>
- [30] Kevin Harris, Lee Green, Juan Garcia, Juan Castro, Juan González. *Intelligent Personal Assistants in Education: Applications and Challenges*. Kuwait Journal of Machine Learning, 2(2). Retrieved from <http://kuwaitjournals.com/index.php/kjml/article/view/185>
- [31] Kumbhkar, M., Shukla, P., Singh, Y., Sangia, R. A., & Dhaliya, D. (2023). Dimensional reduction method based on big data techniques for large scale data. Paper presented at the 2023 IEEE International Conference on Integrated Circuits and Communication Systems, ICICACS 2023, doi:10.1109/ICICACS57338.2023.10100261 Retrieved from www.scopus.com